



# Estimation of extreme precipitations in Estonia and Italy using dual-pol weather radar QPEs

Roberto Cremonini<sup>\*1,3</sup>, Tanel Voormansik<sup>2,4</sup>, Piia Post<sup>2</sup>, and Dmitri Moisseev<sup>3,5</sup>

<sup>1</sup>Department of Physics, University of Helsinki, Finland

<sup>2</sup>Institute of Physics, University of Tartu, Estonia

<sup>3</sup>Regional Agency for Environmental Protection of Piemonte, Department for Natural and Environmental Risks, Torino, Italy

<sup>4</sup>Estonian Environment Agency, Tallinn, Estonia

<sup>5</sup>Finnish Meteorological Institute, Helsinki, Finland

**Correspondence:** Roberto Cremonini (rcremoni@ad.helsinki.fi)

**Abstract.** Climatology of extreme rainfalls for a certain location is commonly taken into account designing stormwater management systems. Rain gauge data have often been used to estimate rainfall intensity for a given return period. However, the poor spatial and temporal resolution of operational gauges is the main limiting factor. Several studies have used rainfall estimates based on weather radar horizontal reflectivity ( $Z_h$ ), but they come with a great caveat: while proven reliable on low or moderate rainfall rates, they are subject to major errors in extreme rainfall and convective cases. It is widely known that C-band weather radar can both underestimate precipitation intensity due to signal attenuation or overestimate it due to hail and clutter contamination. This study circumvents these shortcomings by using specific differential phase ( $K_{dp}$ ) data from dual-polarization C-band weather radars. The rain intensity estimates based on specific differential phase are immune to attenuation and affected less by hail contamination.

This study aims to estimate depth-duration-frequency (DDF) curves computed using polarimetric weather radar data using quantitative precipitation estimations (QPEs) based on  $K_{dp}$  data and to compare the results with the DDF curves derived using rain-gauge data. Only the warm period of the year is here considered, as most of the extreme precipitation events take place at this time. Limiting the dataset to warm period also allows us to use the radar-based rainfall quantitative precipitation estimates, which are more reliable than the snowfall ones. Single C-band polarimetric weather radar site data are used both from Italy and Estonia. This study demonstrates that polarimetric weather radar observations can provide a reliable QPEs compared to rain gauges and, that even relatively short time series can provide a reliable estimation of the rainfall return periods in climatological homogeneous areas.

## 1 Introduction

The increase in impervious surfaces due to urbanization leads to increase in flooding frequency due to poor infiltration and faster concentration time. The hydrological changes, driven by heavy urbanization, and resulting impacts on extreme rainfall,

\*Corresponding author: Roberto Cremonini, Department of Physics, University of Helsinki, Finland, e-mail: rcremoni@ad.helsinki.fi



are also being established: a significant amount of research over the last twenty years has shown a strong relationship between urban areas and local microclimate.

Moreover, as stated by IPCC Fifth Assessment Report (IPCC, 2014), in the near future several Earth regions are likely to be affected by an increase in heavy precipitation events due to climate change (IPCC, 2014). In Europe Besselaar et al. (2012) demonstrated that higher latitudes are yet experiencing an increment in intensity and frequency of extreme events, and correspondingly in heavy precipitations. For all these reasons, studies on extreme annual rainfall maximum depths for short durations are extremely relevant for hydrological studies, water management, and urban areas development (Marra et al., 2017).

However, the reliability of traditional rainfall depths estimations is often limited by the low spatial density of rain gauge networks, particularly for short durations (Overeem et al., 2010). Nevertheless, single-polarization weather radars can provide quantitative precipitation estimates (QPEs), based on  $Z_h - R$  relationships, with proper spatial and temporal resolution. Several studies investigated statistics of extreme areal rainfall depths obtained from single-polarization weather radar (Frederick et al., 1977; Allen et al., 2005b; Overeem et al., 2008, 2009a, b, 2010; Peleg et al., 2016; Marra and Morin, 2015; Panziera et al., 2018). Keupp et al. (2017) and Fabry et al. (2017) offer a complete review of monthly or annual rainfall climatology based on weather radar observations respectively in Europe and the the contiguous United States (CONUS) area.

However, due to signal attenuation at C-band (Delrieu et al., 2000) and due to hail contamination (Ryzhkov et al., 2013), the horizontal radar reflectivity ( $Z_h$ ) is subjected to major errors, especially during intense rainfalls and convective precipitations. As stated by Fairman et al. (2015), relevant underestimations typically can be found in areas of high elevation, far away from the radar, or both; beam blocking and overshooting also cause large differences between QPEs and reference gauges. To overcome these limitations, several adjustment techniques have been developed, correcting QPEs, derived from single-polarization weather radar, with raingauges measurements (Einfalt and Michaelides, 2008; Goudenhoofdt and Delobbe, 2009). Studies like Overeem et al. (2009b) and Peleg et al. (2016) derived short-duration extreme rainfall depths from gauges-adjusted weather radar QPEs. Barndes et al. (2001) and Ryzhkov et al. (2005) demonstrated that polarimetric rainfall estimation algorithms based on specific differential phase ( $K_{dp}$ ) outperform the conventional QPEs based on horizontal radar reflectivity, being immune from partial beam-blocking, attenuation, hail contamination, and weather radar miscalibration. Several studies focused on the evaluation of  $R(K_{dp})$  relationships performances with respect to traditional  $R(Z)$  for precipitation events (Paulitsch et al., 2009; Moisseev et al., 2010; Cremonini and Bechini, 2010). Voormansik et al. (2021a) deeply analyzed five years QPEs derived from operational polarimetric weather radar in Estonia and Italy, demonstrating that  $R(Z_h, K_{dp})$  relationships provide good quality QPEs.

For the first time, this study investigates the statistical properties of annual rainfall maximum for short-durations analyzing QPEs derived from  $R(Z_h, K_{dp})$  observations by operational dual-polarization C-band weather radars in two different climate regions. The results derived from short period weather radar observations are compared with statistics obtained from gauges measurements and QPEs based on traditional horizontal radar reflectivity. Section 2 provides a description of study areas, weather radar systems, and algorithms used to derive QPEs. In Section 3 extreme value statistic is applied to derive depth-duration-frequency (DDF) curves, which describe the rainfall depth as a function of duration for given return periods. Finally, discussion and conclusions follow.



## 2 Materials and methods

This study focuses on QPEs based on polarimetric weather radar, operating in Northern Italy and Estonia. The studied period is limited to the warm period of the year as most of the extreme precipitation events take place at this time. Limiting the dataset to warm period also helps to exclude that weather radar observations come from snow or ice crystals, a requirement for reliable  
60 rainfall intensity estimations based on  $R(Z_h, K_{dp})$ .

### 2.1 The study areas

This study focuses on areas in Piemonte, Italy, and Estonia, covered by operational dual-polarization Doppler C-band weather radars.

Piemonte is located in northwestern Italy, in the upper areas of the Po valley; the central part of the region is relatively flat  
65 (300-200 m a.s.l.) with the Torino hill that reaches 770 meters a.s.l.. The Alps surround plains with altitudes ranging from 1,000 m to more than 4,500 m a.s.l.. The two areas considered in this study are centered on Torino hill and they extend for about 40 km far from the weather radar, corresponding to about  $7,300 \text{ km}^2$  altogether (Figure 1). To ensure QPEs data quality, the choice to restrict the study areas close to the radar site is driven by these main reasons:

1. to reduce weather radar beam-broadening and beam propagation effects;
- 70 2. to avoid the Alps complex orography in western and northern directions;
3. to limit the weather radar beam height above ground.

The Piemonte rainfall regime is sub-continental with a dry season during winter, the main maximum precipitation occurs during fall and a secondary maximum during spring-summer (Devoli et al., 2018); convective precipitations are very frequent from late spring to early fall. Pavan et al. (2018) reconstructed rainfall climatology over Po valley from gauges observations  
75 from 1961 to 2015, showing that, although the relatively small extent of the study areas, there are different precipitation regimes between areas located close to the Alps (wetter) and the flats south of Torino hill (drier).

The Bric della Croce weather radar, operated by the regional agency for environment protection (Arpa Piemonte) is located on the top of Torino hill. The operational radar completes fully polarimetric volume scans, made of eleven elevations up to 170 km range with 340 m range bin resolution. Quantitative precipitation estimates (QPEs), based on horizontal reflectivity,  
80 are extensively described by Cremonini and Tiranti (2018), meanwhile,  $K_{dp}$  precipitation estimations are derived according to Wang and Chandrasekar (2009). The closest observations to the weather radar (up to eight kilometers) have been left out due to heavy ground clutter contamination and unreliable estimations of  $K_{dp}$ . Being focused on convective precipitation, this study limits the analysis to the warm season ranging in Italy from April to October.

Bric della Croce data range from 2014 to 2020 with five minutes interval time resolution.

85 The data inspection for quality purposes has shown that the annual maxima for the years 2015 and 2016 are unreliable, due to frequent weather radar failures during the warm season: for this reason, these years have been excluded from the following analysis.

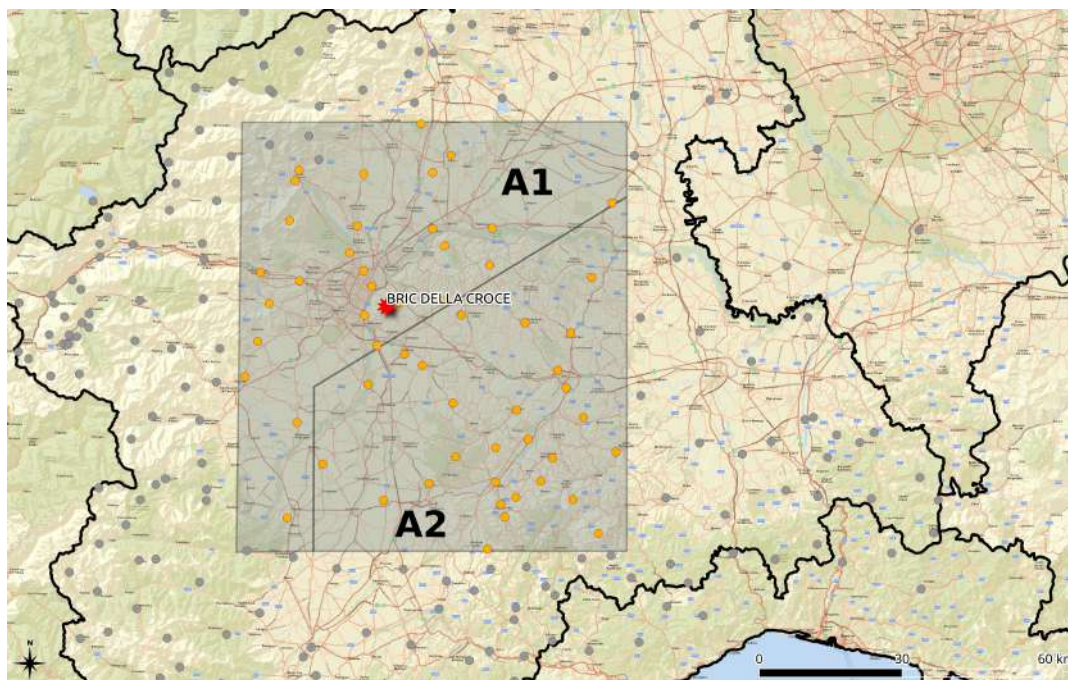


**Figure 1.** The two Italian study areas: dots tipping-bucket raingauges of the regional hydrological network, orange dots tipping-bucket raingauges used in the study, the red star is the Bric della Croce radar site; basemap: ESRI, [https://basemaps.arcgis.com/arcgis/rest/services/World\\_Basemap\\_v2/VectorTileServer](https://basemaps.arcgis.com/arcgis/rest/services/World_Basemap_v2/VectorTileServer) accessed on 5 August 2022

Arpa Piemonte also operates an automated ground weather network made by more than 350 raingauges with 0.2 mm resolution and 300 mm/h maximum detectable rainfall intensity: one-minute rainfall observations are available since 1988. Annual hourly rainfall maxima are derived from gauges observations corrected for underestimations at high rainfall intensities according to Lanza et al. (2010); Vuerich (2009). Annual hourly rainfall maxima are manually quality controlled to identify possible mechanical failures and incomplete time-series. In this work, one-minute resolution tipping-bucket raingauges located within the two study areas and running for at least 15 years have been used. Area 1 (A1) north and west of the weather radar site contains 27 gauges, while Area 2 (A2) contains 25 gauges; the annual hourly precipitation maxima range from 1988 to 2020. Annual precipitation maxima derived from raingauges confirm different precipitation regimes in A1 and A2.

The study area in Estonia is centered on the continental part of the country and it extends for about 70 km around the radar corresponding to 16,911 km<sup>2</sup>. Estonia is a flat country with a mean elevation of about 50 m a.s.l. and the highest point being 318 m a.s.l in the more hilly southeast (Figure 2). Estonia has a temperate climate with the heaviest rainfall in late summer. Convective precipitation is common in the area from May to September (Voormansik et al., 2021b). There are distinct differences in precipitation climate between continental Estonia and the coastal areas and islands as the latter is much drier



(Tammets and Jaagus, 2013). This variance is caused by different thermal regimes of sea and land surfaces. In the study area, we can thus expect a uniform precipitation regime.

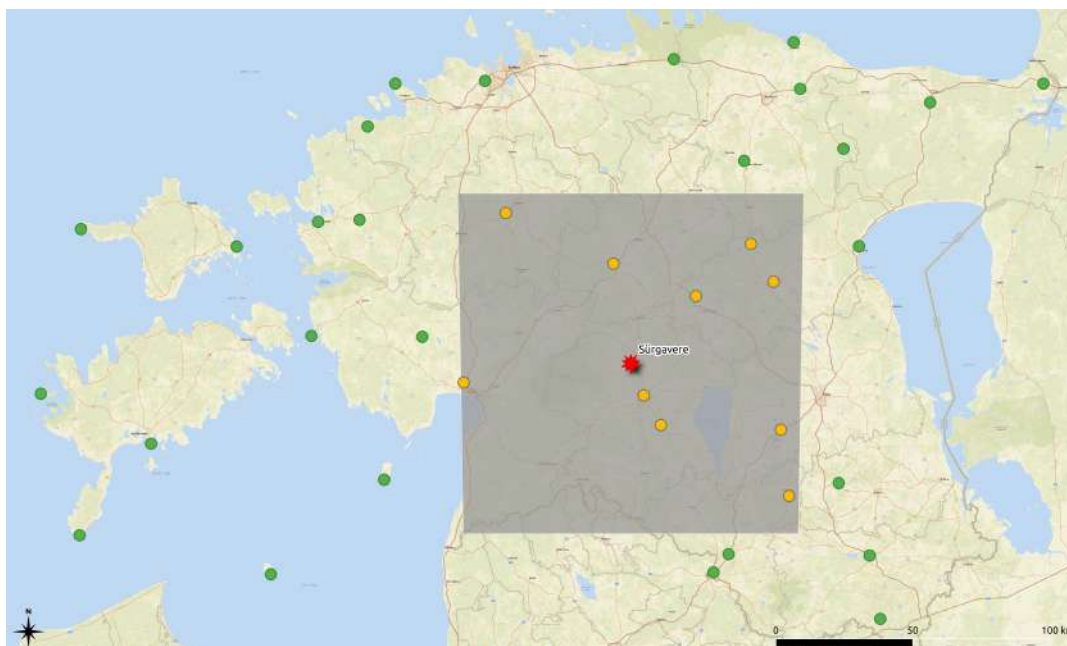


**Figure 2.** The Estonian study area (shaded): the dots are weighted rain gauges of the regional hydrological network, the orange dots are weighted rain gauges used in the study, and the pink star Sürgavere radar location; basemap: ESRI, [https://basemaps.arcgis.com/arcgis/rest/services/World\\_Basemap\\_v2/VectorTileServer](https://basemaps.arcgis.com/arcgis/rest/services/World_Basemap_v2/VectorTileServer) accessed on 5 August 2022

105 Sürgavere radar is situated in the northern part of Sakala upland on top of Sürgavere hill (128 m a.s.l.). Sürgavere radar has been operational since 2008 and a continuous archive is available since 2010. Until May 2020, the radar performed a volume scan with eight elevations up to 250 km range with 300 m range bin resolution every 15 minutes. In May 2020 the scan strategy received a major update. Since then the radar scans seven elevations with a 250 km range every five minutes and the lowest elevation with a 250 km range every 2.5 minutes. After careful inspection of reflectivity and polarimetric data quality, five  
110 years of radar data (2012-2013 and 2018-2020) were included in the study. Data from 2014, 2015, and 2017 were not included because of insufficient polarimetric data quality to obtain reliable QPEs. 2014 and 2015 were excluded because of a broken waveguide limiter which caused gradually decreasing polarimetric data quality. Data from 2017 was left out because a broken stable local oscillator (STALO) reduced the data quality to levels not usable for QPE purposes. The year 2016 was omitted because of the low availability of radar data due to frequent and long-lasting radar failures (availability of 30% for August and  
115 85% for the whole summer period of that year) that would result in unreliable annual maxima. Mean radar data availability for the investigated five year period was 98%. Only 15-minutes interval data is used in this study to maintain homogeneity.

$K_{dp}$  precipitation estimates of Estonia are derived using PyART function *phase\_proc\_lp* (Giangrande et al., 2013). Compared to the work by Voormansik et al. (2021a) done in the same study area some parameters of this function have been changed. The



necessity of updating the parameters became inevitable because using the parameters of the earlier work led to unrealistically  
120 high 1-hour rainfall maxima and over smoothed precipitation fields. The parameters of the function that were changed were  
*window\_len*, *high\_z*, and *coeff*. The first of these, *window\_len*, allows changing the length of the Sobel window applied to  $\Phi_{dp}$   
field before calculating  $K_{dp}$ . When using the default window length of 35, the function produces less accurate results in  $K_{dp}$   
fields with steep gradients and large  $K_{dp}$  magnitudes as it oversmooths the  $\Phi_{dp}$  field (Reimel and Kumjian, 2021). We tested  
with various window lengths and found length 8 to be the optimal compromise between spatial resolution and smoothness.  
125 After the window length change, we obtained realistic looking precipitation fields but the overestimation compared to gauge  
values increased. This is because  $\Phi_{dp}$  gradients became steeper as a result of the smaller window length. To mitigate this issue  
we first decreased the *high\_z* (high limit for reflectivity to remove hail contamination) value from 60 dBZ used in Voormansik  
et al. (2021a) to 50 dBZ which is the lowest recommended value by Giangrande et al. (2013). Because overestimation was still  
evident we also reduced the  $Z_h$ - $K_{dp}$  self-consistency coefficient. As stated by Kumjian et al. (2019) the  $Z_h$ - $K_{dp}$  consistency  
130 relationships probably do not exist in hail and it is therefore recommended to reduce the weight of the self-consistency con-  
straint in the case of hail (Reimel and Kumjian, 2021). We tested with various values and found the coefficient value of 0.9 to  
produce the optimal results.

The following equations have been used to derive rain rate from weather radar variables:

$$135 \quad R(Z_h) = 300Z^{1.5} \quad (1)$$

and

$$R(K_{dp}) = 21.0K_{dp}^{0.720} \quad (2)$$

Horizontal reflectivity data is re-calibrated using a method that makes use of the knowledge that  $Z_h$ ,  $Z_{dr}$  (differential  
reflectivity), and  $K_{dp}$  are self-consistent with one another and one can be computed from two of the others. The calibration  
140 was carried out using the theory set down in Gorgucci et al. (1992) and Gourley et al. (2009) where the process is described in  
detail. As a result,  $Z_h$  bias of 2.0 to 5.0 dB depending on the data period is obtained and added to the corresponding original  
reflectivity data. Data up to 10 km from the radar were excluded because of the ground clutter and unreliable  $K_{dp}$  estimation.  
Weighted rain gauges operated by the Estonian Environment Agency (EstEA) located in the study area are used as ground  
truth to compare with radar estimates. The rain gauges provide data with a resolution of 0.1 mm and maximum detectable  
145 rainfall intensity of 2000 mm/h. Rainfall observations from 2003-2010 are available with 1-hour resolution and starting from  
2011 with 10-minutes interval. The data are manually quality controlled by EstEA staff to identify possible technical issues  
or incomplete time series. In this study ten years of gauge data from 10 stations located in the study area from 2011 to 2020  
are used. As demonstrated by Voormansik et al. (2021a), the combined product  $R(Z_h, K_{dp})$  outperforms with respect to QPEs  
based on  $R(Z_h)$  and  $R(K_{dp})$ . The weather radar-based QPE here used is defined as:



$$150 \quad R(Z_h, K_{dp}) = \begin{cases} R(Z_h), & \text{if } Z_h \leq 25 \text{ dBZ} \\ R(K_{dp}), & \text{otherwise} \end{cases} \quad (3)$$

The evaluation of reflectivity threshold has been derived optimizing results on 1-hour accumulation rainfall in both locations, Italy and Estonia.

### 2.1.1 GEV Statistics

155 Extreme value theory (EVT) deals with the stochasticity of natural variability by describing extreme events concerning a probability of occurrence. The frequency of occurrence for events with varying magnitudes can be described as a series of identically distributed random variables

$$F = X_1, X_2, X_3, \dots, X_N \quad (4)$$

where  $F$  is some function that approximates the relationship between the magnitude of the event (variable  $X_N$ ) and the probability of its occurrence. EVT is one of the most recurrent methodologies used for the statistical description of rare events. 160 Extensive literature, dating back to the 1940s, deals with EVT in its formalization and its hydrological applications. Looking at the distribution of block maxima (a block is defined as a set period such as a year), the Generalized Extreme Value (GEV) distribution is one of the most popular fundamental approaches: the introduction theory and a historical review on this topic can be found in Papalexiou et al. (2013), Wilks (2011), de Haan and Ferreira (2006). According to Katz et al. (2002), the GEV distribution, which combines three different statistical families (Gumbel, Fréchet, and Weibull), can fit the extreme data set 165 with high accuracy.

Defining  $R_{1h}$  as the random variable of annual maximum rainfall intensity for the hourly duration, it is expected that random samples of annual maxima are distributed as the GEV cumulative distribution function  $F(x)$  (Jenkinson, 1955):

$$F(R_{1h} \leq x; \mu, \sigma, \xi) = \begin{cases} e^{-[1+\xi \frac{x-\mu}{\sigma}]^{\frac{1}{\xi}}} & \xi \neq 0 \\ e^{-e^{-\frac{x-\mu}{\sigma}}} & \xi = 0 \end{cases} \quad (5)$$

170 where three parameters,  $\mu$ ,  $\sigma$  and  $\xi$  represent respectively the location, scale, and shape of the distribution function. Note that  $\sigma$  and  $1 + \xi(x - \mu)/\sigma$  must be greater than zero, while the shape and location parameters can take on any real value. The shape parameter  $\xi$  governs the three limiting distributions of extreme values:

- $\xi > 0$  Fréchet distribution (EV2);
- $\xi = 0$  Gumbel distribution (EV1);



–  $\xi < 0$  Weibull distribution (EV3).

175 Several methods have been developed for the estimation of GEV distribution parameters, including the method of moments (MME), the method of L-moments (LME), the method of probability-weighted moments (PWME), and the method of maximum likelihood (MLE) (Katz et al., 2002; de Haan and Ferreira, 2006). Hereafter, the only MLE method has been used to estimate GEV distribution parameters from sample data.

180 Quantiles associated with the  $T$ -year return period  $T = 1/1 - F(r_{1h} \leq x)$  are determined by inverting the GEV cumulative distribution function given by Eq. (5).

As stated by Lazoglou et al. (2018), the Weibull (negative shape parameter) is not appropriate for precipitation datasets. Moreover, Ragulina and Reitan (2017) demonstrated that small countries or administrative regions within larger countries can be assigned roughly the same shape parameter, but larger areas such as continents can be expected to be heterogeneous. As a result of their work, which considered 1,495 stations worldwide, the global average for the shape parameter is equal to 0.139, with a 99% credibility interval ranging from 0.127 to 0.150. The weather radar-based rainfall annual maxima statistics over the Netherlands calculated by Overeem et al. (2009a) have shown that regional differences in the GEV location parameter exist for the most duration. Nevertheless, due to the small number of rainfall annual maxima, when depth-duration-frequency (DDF) curves are derived for small areas, the uncertainties in the DDF curves generally become larger compared to the uncertainties of the average DDF curve for the Netherlands. Moreover, as discussed by Overeem et al. (2009a), the spatial correlation of measurements affects extreme values statistics, carrying to underestimation. The correlation between two raingauges is typically low for convective precipitation, due to the small spatial scales involved in convection ( $\approx 10 - 100 \text{ km}^2$ ) and the low density of the ground meteorological network (typically order of one gauge every  $100 \text{ km}^2$ ). In the case of weather radar observations, given the higher spatial resolution ( $\approx 1 \text{ km}^2$ ), the correlation between close cell grids must be estimated and taken into account. In this study, the statistical analysis has been conducted using the R (<https://cran.r-project.org/>) package ExtRemes 2.1 (Gilleland et al., 2016).

### 3 Results

Assuming GEV distribution parameters are constant in each of area considered in this study, their estimation from all data in the regions justifies the derivation of return periods longer than the rainfall record (Overeem et al., 2010). This statement assumes that both sample data are independent and the precipitation regime in the studied area is uniform. Semi-variograms are widely used in geostatistic sciences for evaluating rainfall spatial structure. Semi-variograms summarize the spatial relations in the data, and they can be used to understand within what range data are spatially correlated (Naimi et al., 2011). The experimental isotropic semi-variogram can be derived by taking half the average of the squared difference between data pairs at equal distances and by assuming stationarity and isotropy of the rainfall field (Cressie, 1993):

$$\gamma(h) = \frac{1}{2n(|h|)} \sum_{k=1}^{n(|h|)} (z(x_k + h) - z(x_k))^2 \quad (6)$$





205 where  $x_k$  is the location of cell barycentre  $k$  and  $x_k + h$  is the location at distance  $h$  from location  $x_k$ .

Figure ?? shows semi-variograms, obtained from  $Z - K_{dp}$  annual hourly rainfall maxima, from April to September in Italy for Area 1 (left) and Estonia (right).

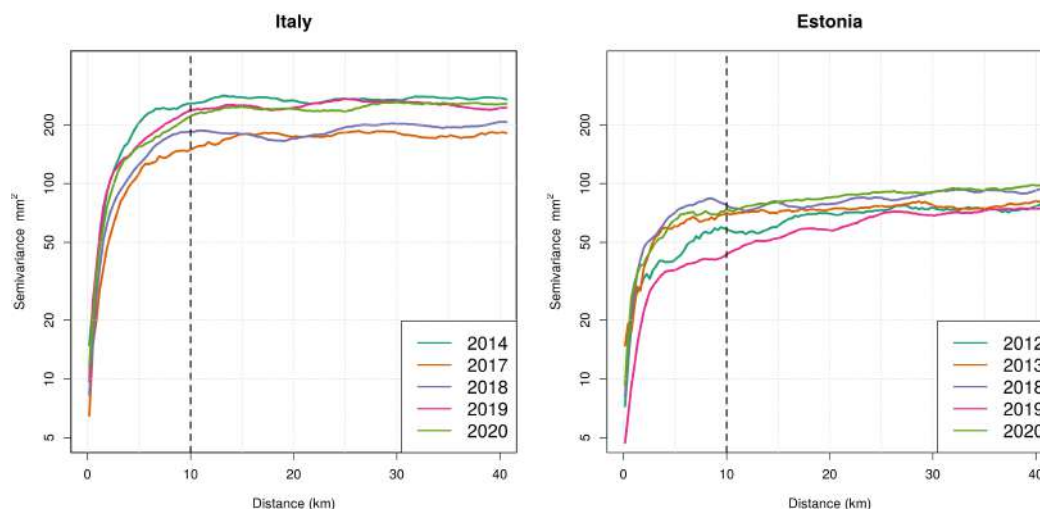


**Figure 3.** Empirical variograms for hourly rainfall annual maxima based on  $Z - K_{dp}$  hourly rainfall estimations in Italy Area 1 (left) and Estonia (right).

The empirical semi-variogram analysis for weather radar observations indicates that hourly rainfall maxima decorrelate at  
210 about 10 km both in Estonia and Italy (Figure 3). These results are consistent with past studies (Schroerer et al., 2018; Dzotsi  
et al., 2012): convective precipitation is prevalent during the warm season and, consequently, the spatial correlation quickly  
decreases with the distance between two rain gauges. Moreover, ten kilometers is the typical spatial scale of convective precip-  
itation systems (*meso* –  $\gamma$ ). Different values of semi-variances in Estonia and Italy can be explained by the different climatic  
regimes, with generally weaker convective precipitations in the Baltic country. Hence, to avoid statistical oversampling and  
215 to ensure statistical independence of data samples, one-hour precipitations annual maxima estimated by weather radar are  
re-sampled according to the found spatial scale of convective precipitation. The hourly annual rainfall maxima estimated by  
weather radar observations are up-scaled from the original data resolution (340 meters for Italy and 300 meters for Estonia) to  
10 km resolution, using a uniform random sampling algorithm.

The GEV distribution unites the Gumbel, Fréchet, and Weibull distributions into a single family to allow a continuous range  
220 of possible shapes (Früh et al., 2010; Coles, 2001). These three distributions are known as type I, II, and III extreme value dis-  
tributions. The GEV distribution is parameterized with a location parameter ( $\mu$ ), scale parameter ( $\sigma > 0$ ), and shape parameter  
( $\xi$ ). The GEV is equivalent to type I, II, and III, respectively, when a shape parameter is equal to zero, greater than zero, and  
lower than zero. Based on the extreme value theorem, the GEV distribution is the limit distribution of properly normalized



maxima of a sequence of independent and identically distributed random variables. Thus, the GEV distribution is used as an  
225 approximation to model the maxima of long (finite) sequences of random variables.

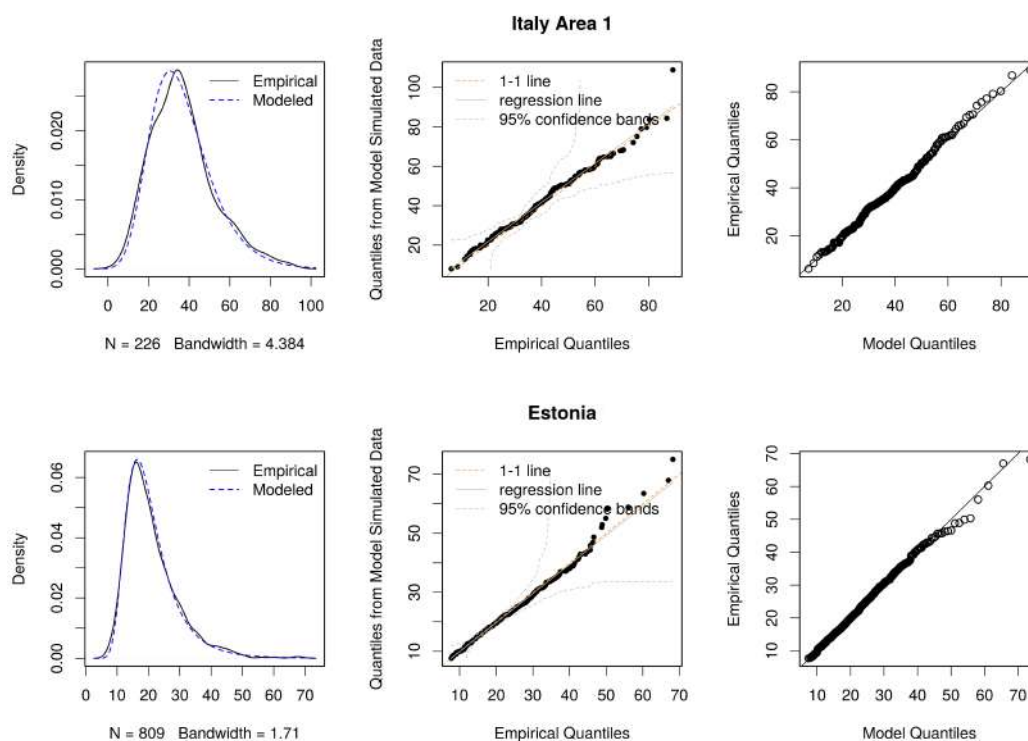


**Figure 4.** Diagnostic plots for 1-hour annual rainfall maxima fits derived by weather radar in Italy Area 1 (upper) and Estonia (lower): from left to right, density plot of the data along with the model fitted density, Q-Q plot of the data quantiles against the fitted model quantiles with 95% confidence bands, a Q-Q plot of quantiles from model-simulated data against the data.

Figure 4 shows the diagnostics from the GEV distribution fitted to 1-hour rainfall annual maxima in Italy for Area 1 (upper) and Estonia (lower); from left to right, the Figure shows the density plot of the data along with the model fitted density, the Q-Q  
230 plot of the data quantiles against the fitted model quantiles with 95% confidence bands, a Q-Q plot of quantiles from model-simulated data against the data. Quantile-quantile scatterplots compare empirical data and fitted CDFs in terms of quantiles:  
in an ideal perfect fitting, all points should lay on the 1:1 diagonal line (Wilks, 2011). The Q-Q plots present some departures  
from linearity in correspondence of the tails, especially for Estonia data, which are due to the increasing level of uncertainty  
that characterizes model extrapolation at high levels. The empirical estimates in the return level plot reflect results in Q-Q plots  
laying very close to the model-based line, which results be almost linear, for low values. However, even if the return level  
estimates seem convincing, the increasing confidence bands for large return periods indicate the uncertainty that affects the  
235 model at high levels.



Area	Source	$\mu$ (mm)	$\sigma$	$\xi$	n-values
Italy - A1	WR	$34.5 \pm 1.0$	$14.5 \pm 0.8$	$0.08 \pm 0.04$	226
	RG	$29.9 \pm 0.5$	$11.1 \pm 0.4$	$-0.009 \pm 0.006$	609
Italy - A2	WR	$27.6 \pm 0.9$	$11.4 \pm 0.6$	$-0.08 \pm 0.06$	235
	RG	$24.9 \pm 0.4$	$9.6 \pm 0.3$	$0.005 \pm 0.03$	595
Estonia	WR	$17.0 \pm 0.2$	$5.6 \pm 0.2$	$0.12 \pm 0.02$	809
	RG	$15.2 \pm 0.7$	$5.9 \pm 0.5$	$-0.02 \pm 0.07$	93

**Table 1.** Estimated GEV parameters, location, scale, and shape ( $\mu, \sigma, \xi$ ) for weather radar and gauges annual hourly maxima rainfall intensities for Italy Area 1 and Area 2 and Estonia for weather radar (WR) and raingauges (RG) time-series observations

Table 1 summarizes the results of fitting data samples with GEV distribution by applying the Maximum Likelihood Estimation method (MLE) for each studied area. Values for location, scale, and shape parameters with their standard deviations are shown. Most of the shape parameters are close to zero, indicating a theoretical Gumbel distribution as expected. Significant exceptions are the negative value for study area 1 in Italy for GEV fit derived by rain gauges, and the positive value for Estonia fit derived from the weather radar.

The record length strongly affects the estimate of the GEV shape parameter and long historical time series are needed for reliable estimates. Papalexiou et al. (2013), Ragulina and Reitan (2017), Lazoglou et al. (2018), Deidda et al. (2021) demonstrated that the shape parameter tends to have positive values, between 0 and 0.23 with a probability of 99%, as sample size increases. For Estonia, the shape parameter  $\xi$  positive ( $+0.12 \pm 0.02$ ) derived from weather radar agrees with findings in the extreme value rainfall analysis of these studies (Ragulina and Reitan, 2017). On the other side, close to zero values for shape parameters estimated by Italian weather radar observations can be explained by the limited sample size.

#### 4 Discussion

Several studies developed adjustment techniques to correct QPEs based on weather radar observations with rain gauges measurements (Einfalt and Michaelides, 2008; Goudenhoofdt and Delobbe, 2009). For the first time, this study investigates extreme precipitation estimation using dual-pol weather radar rainfall estimations without any adjustment with raingauges. It is worth recalling that the study has been limited to relatively flat areas with highquality weather radar observations close to the ground. Data quality and reliability have been carefully checked in Voormansik et al. (2021a).

The two studied regions, Estonia and Italy, are characterized by different precipitation regimes, colder the first one and warmer the latter. The different climate regimes of studied areas consequently reflect on GEV distribution estimations, determining lower return periods in Italy, given hourly precipitations. Estonia is characterized by few rain gauges and by a limited historical series, but also by a larger homogeneous flat region covered by the operational polarimetric weather radar. In this area, it can be appreciated the benefit of estimating GEV distribution using weather radar observations: the sample size derived from five years observations is made by 809 values, about nine times the sample size obtained by raingauges. These different sample



sizes determine larger standard deviations in GEV distribution parameters estimation by raingauges with respect to weather  
260 radar-based estimation.

In Italy, an opposite condition is evident: a dense automatic gauges network is operating since 1988, providing about 30 gauges  
per area and more than 600 values in sample size. But, the Alps and the spatial variability of the climate regime, influenced  
by complex orography, limit the available weather radar observations to about 250 values. Despite the limited availability of  
weather radar observations (only five years for both Italian and Estonian weather radars), the comparison of GEV distribution  
265 fits in these two different regions has shown encouraging results.

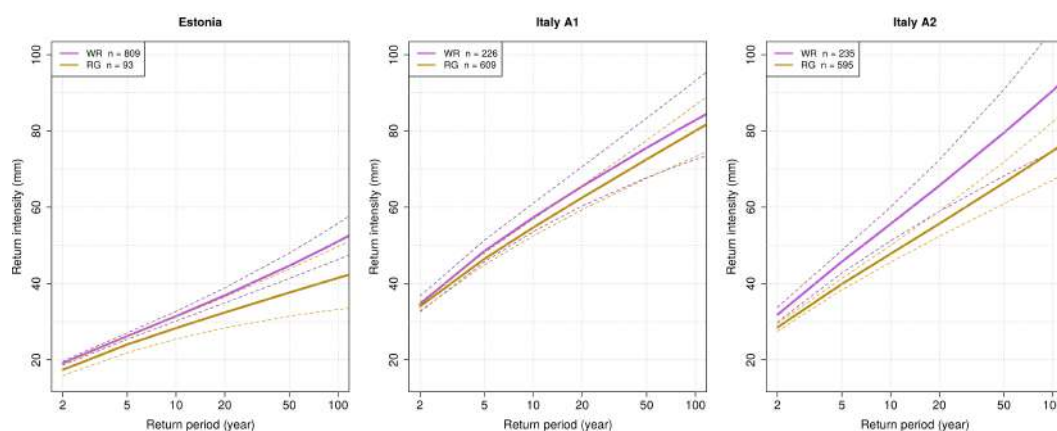


**Figure 5.** Return levels for 1-hour rainfall accumulation in Estonia (left) and Italy Area 1 (center) and Area 2 (right).

Figure 5 shows return levels for 1-hour rainfall at a given return time, estimated from GEV distributions with location, shape,  
and scale parameters from Table 1. In Italy, the different return periods between the two areas are in agreement with findings  
reported by Pavan et al. (2018), with Area 1 more favorable to intense precipitation than Area 2. This condition, confirmed  
also by climatological lightning density (not shown), is caused by local orography. In fact, during the warm season, cold air  
270 overcomes the Alps flowing towards the Po valley from west-northwest: the Monferrato hills east of Torino enhance lowlevel  
convergences and strong uplifts, causing deep convection in Area 1. QPEs based on  $Z_h - K_{dp}$  generally provided shorter return  
periods with respect to gauges estimations, probably due to a slight overestimation of annual rainfall maxima by weather radars,  
as highlighted by Voormansik et al. (2021a).

## 5 Conclusions

275 Several studies investigated rainfall annual maxima derived from weather radarbased QPEs obtained by the traditional  $Z_h - R$   
relationship with some adjustments with raingauges. Nevertheless, as stated by Bringi and Chandrasekhar (2001) and Voor-  
mansik et al. (2021a), the benefits of using  $K_{dp}$  in rainfall estimates are evident: these QPEs are immune from weather radar  
miscalibration, anomalous propagation, and partial beam blockings.



For the first time, this study investigates QPEs based on polarimetric observations by operational C-band weather radar located  
280 in Italy and Estonia. As shown by Voormansik et al. (2021a), rainfall estimations based on  $Z_h - K_{dp}$  are robust and reliable, overcoming most of the sources' uncertainties: hence, no corrections nor adjustments with raingauges have been applied. The annual maximum of one hour rainfall accumulation is typically assumed to have extreme value (GEV) distribution. Hence, GEV distribution parameters and depth-duration-frequency curves have been derived from the one-hour dual-pol weather radar-based annual rainfall maxima. The comparison of weather radar return period estimations with ones derived from longterm  
285 gauges observations showed a good agreement. Moreover, this study demonstrates that thanks to weather radar's high spatial resolution, even a limited time series of weather radar observations can provide reliable estimations of extreme values distribution parameters for annual hourly rainfall maxima in climatological homogeneous regions. It is worth recalling that QPEs based on  $Z_h - K_{dp}$  observations can be obtained only in cases of warm season precipitations (anyway, when most intense precipitations occur). The shown results demonstrate good agreement between weather radar and raingauges data and consistent  
290 estimations of GEV distribution parameters. Moreover, this study shows that even limited time-series weather radar observations can discriminate between different precipitation regimes. These results are promising especially if we recall that the two areas in Italy are characterized by slightly different precipitation regimes and the applied statistical analysis can describe them properly. The main requirements applying this approach consist of a proper weather radar calibration, radar visibility, and a limited beam-broadening united to weather observations close to the ground.  
295 Sub-hourly precipitation extremes can determine a wide range of impacts on infrastructure, economy, and even health causing urban flooding, triggering landslides, flash floods, and heavy soil erosion. Hence, future works will investigate sub-hourly rainfall accumulation intervals, estimating GEV parameter distributions and deriving significant return periods.

*Code and data availability.* The code used to conduct all analyses, raingauges and weather radar data used in this study are available by contacting the authors.

300 *Author contributions.* R.C., T.V., D.M. and P.P. contributed to the design and implementation of the research, to the analysis of the results and to the writing of the manuscript. All authors read and approved the manuscript.

*Competing interests.* The authors declare no conflict of interest.

*Acknowledgements.* This research has been supported by the Estonian Research Council (grant no. PSG202). All figures included in the study were produced by the use of Free and Open Source Software (i.e. Quantum GIS Geographic Information System - Open Source  
305 Geospatial Foundation Project, <http://qgis.osgeo.org>, and the R Project for Statistical Computing, <https://www.R-project.org/>).



## References

- Allen, R. J., and A. T. De Gaetano (2005b), Considerations for the use of radar-derived precipitation estimates in determining return intervals for extreme areal precipitation amounts, *J. Hydrol.*, 315, 203–219, doi:10.1016/j.jhydrol.2005.03.028.
- Coles, S (2001): *An Introduction to Statistical Modeling of Extreme Values*. Springer Series in Statistics. Springer Verlag London. 208p
- 310 Delrieu, G., Andrieu, H. and Creutin, J.D. (2000). Quantification of path-integrated attenuation for X-and C-band weather radar systems operating in Mediterranean heavy rainfall. *Journal of Applied Meteorology*, 39(6), pp.840-850.
- Brandes, E. A., A. V. Ryzhkov, and D. S. Zrníc, 2001: An evaluation of radar rainfall estimates from specific differential phase. *J. Atmos. Oceanic Technol.*, 18, 363–375, doi:10.1175/1520-0426(2001)018<0363:AEORRE.2.0.CO;2
- Bringi, V. N. and Chandrasekhar, V.: *Polarimetric Doppler Weather Radar. Principles and Applications*. Cambridge University Press, NY,  
315 636 pp., 2001.
- Cressie, N. A.: *Statistics for spatial data*, Wiley, NY, revised edn., 1993. 2090
- Cremonini, R. and Bechini, R. Heavy rainfall monitoring by polarimetric C-Band weather radars. *Water* 2010, 2, 838-848.
- Cremonini, R. and Tiranti, D. (2018) The Weather Radar Observations Applied to Shallow Landslides Prediction: A Case  
Study From North-Western Italy, *Frontiers in Earth Science*, 6, 134, <https://www.frontiersin.org/article/10.3389/feart.2018.00134>,  
320 doi:10.3389/feart.2018.00134,ISSN:2296-6463
- Deidda, R., Hellies, M. and Langousis, A. A critical analysis of the shortcomings in spatial frequency analysis of rainfall extremes based on homogeneous regions and a comparison with a hierarchical boundaryless approach. *Stoch Environ Res Risk Assess* (2021). <https://doi.org/10.1007/s00477-021-02008-x>
- Devoli, G., Tiranti, D., Cremonini, R., Sund, M., and Boje, S.: Comparison of landslide forecasting services in Piedmont (Italy) and Norway, illustrated by events in late spring 2013, *Nat. Hazards Earth Syst. Sci.*, 18, 1351-1372, <https://doi.org/10.5194/nhess-18-1351-2018>, 2018.
- 325 Dzotsi, K. A., Matyas, C. J., Jones, J. W., Baigorria, G., and Hoogenboom, G. (2014). Understanding high resolution space-time variability of rainfall in southwest georgia, United States. *International Journal of Climatology*, 34(11), 3188–3203. <https://doi.org/10.1002/joc.3904>
- E.J.M. van den Besselaar, A.M.G. Klein Tank, T.A. Buishand Trends in European precipitation extremes over 1951-2010 *Int. J. Climatol.* 2689 (2012), 10.1002/joc.3619
- 330 Einfalt, Thomas and Michaelides, Silas. (2008). *Precipitation: Advances in Measurement, Estimation and Prediction*. 10.1007/978-3-540-77655-0\_5.
- Fabry, F., V. Meunier, B.P. Treserras, A. Cournoyer, and B. Nelson, 2017: On the Climatological Use of Radar Data Mosaics: Possibilities and Challenges. *Bull. Amer. Meteor. Soc.*, 98, 2135–2148, <https://doi.org/10.1175/BAMS-D-15-00256.1>
- Fairman, J. G., Jr., D. M. Schultz, D. J. Kirshbaum, S. L. Gray, and A. I. Barrett, 2015: A radar-based rainfall climatology of Great Britain  
335 and Ireland. *Weather*, 70, 153–158, doi:<https://doi.org/10.1002/wea.2486>
- Frederick, R. H., V. A. Myers, and E. P. Auciello (1977), Storm depth-area relations from digitized radar returns, *Water Resour. Res.*, 13, 675–679, doi:10.1029/WR013i003p00675.
- Früh, B., H. Feldmann, H.-J. Panitz, and G. Schädler, D. Jacob, P. Lorenz, and K. Keuler, 2010: Determination of precipitation return values in complex terrain and their evaluation. *J. Climate*, 23, 2257–2274.
- 340 Gilleland E, Katz RW (2016). ExtRemes 2.0: An Extreme Value Analysis Package in R, *Journal of Statistical Software*, 72(8), 1–39. doi:10.18637/jss.v072.i08.



- Giangrande, S.E., McGraw, R. and Lei, L. (2013). An application of linear programming to polarimetric radar differential phase processing. *Journal of Atmospheric and Ocean Technology*, 30(8), pp.1716-1729.
- Gorgucci, E., Sarchilli, G., and Chandrasekar, V. (1992). Calibration of radars using polarimetric techniques. *IEEE transactions on geo-*  
345 *science and remote sensing*, 30(5), 853-858.
- Goudenhoofdt, E. and Delobbe, L.: Evaluation of radar-gauge merging methods for quantitative precipitation estimates, *Hydrol. Earth Syst. Sci.*, 13, 195–203, doi:10.5194/hess-13-195- 2009, 2009.
- Gourley, J. J., Illingworth, A. J., and Tabary, P. (2009). Absolute calibration of radar reflectivity using redundancy of the polarization obser-  
vations and implied constraints on drop shapes. *Journal of Atmospheric and Oceanic Technology*, 26(4), 689-703.
- 350 de Haan, L. and Ferreira, A. (2006) *Extreme Value Theory: An Introduction*. Springer, New York. <http://dx.doi.org/10.1007/0-387-34471-3>
- Katz, R.W.; Parlange, M.B.; Naveau, P. Statistics of extremes in hydrology. *Adv. Water Resour.* 2002, 25, 1287–1304.
- Keupp, L.; Winterrath, T.; Hollmann, R. Use of Weather Radar Data for Climate Data Records in WMO Regions IV and VI; Technical  
Report, WMO CCI TT-URSDCM; WMO: Geneva, Switzerland, 2017.
- Kumjian, M.R., Lebo, Z.J. and Ward, A.M., 2019. Storms producing large accumulations of small hail. *Journal of Applied Meteorology and*  
355 *Climatology*, 58(2), pp.341-364.
- IPCC, 2014: *Climate Change 2014: Synthesis Report*. Contribution of Working Groups I, II and III to the Fifth Assessment Report of the  
Intergovernmental Panel on Climate Change [Core Writing Team, R.K. Pachauri and L.A. Meyer (eds.)]. IPCC, Geneva, Switzerland, 151  
pp.
- Jenkinson, A. F. (1955), The frequency distribution of the annual maximum (or minimum) values of meteorological elements, *Quart. J. R.*  
360 *Meteorol. Soc.*, 81, 158 – 171.
- Lanza, L. G., Vuerich, E., and Gnecco, I.: Analysis of highly accurate rain intensity measurements from a field test site, *Adv. Geosci.*, 25,  
37–44, <https://doi.org/10.5194/adgeo-25-37-2010>, 2010.
- Lazoglou, Georgia and Anagnostopoulou, Chr and Tolika, K and Kolyva-Machera, Fotini. (2018). A review of statistical methods to analyze  
extreme precipitation and temperature events in the Mediterranean region. *Theoretical and Applied Climatology*. 10.1007/s00704-018-  
365 2467-8.
- Lutz, J.; Grinde, L.; Dyrddal, A.V. Estimating Rainfall Design Values for the City of Oslo, Norway—Comparison of Methods and Quantifi-  
cation of Uncertainty. *Water* 2020, 12, 1735. <https://doi.org/10.3390/w120617350>
- Marra F., Morin E., Use of radar QPE for the derivation of Intensity–Duration–Frequency curves in a range of climatic regimes, *Journal of*  
*Hydrology*, Volume 531, Part 2, 2015, Pages 427-440, ISSN 0022-1694, <https://doi.org/10.1016/j.jhydrol.2015.08.064>.
- 370 Marra, F., Morin, E., Peleg, N., Mei, Y., and Anagnostou, E. N.: Intensity–duration–frequency curves from remote sensing rainfall estimates:  
comparing satellite and weather radar over the eastern Mediterranean, *Hydrol. Earth Syst. Sci.*, 21, 2389–2404, <https://doi.org/10.5194/hess-21-2389-2017>, 2017.
- Moisseev D., Keränen R., Puhakka P., Salmivaara J., Leskinen M. 2010: Analysis of dual-polarization antenna performance and its effect on  
QPE, 6th European Conference on Radar in Meteorology and Hydrology, Sibiu, Romania;
- 375 Naimi, B., Skidmore, A.K, Groen, T.A., Hamm, N.A.S. 2011. Spatial autocorrelation in predictors reduces the impact of positional uncer-  
tainty in occurrence data on species distribution modelling, *Journal of biogeography*. 38: 1497-1509.
- Overeem, Aart and Buishand, Adri and Holleman, Iwan. (2008). Rainfall depth-duration-frequency curves and their uncertainties. *Journal of*  
*Hydrology*. 348. 124-134. 10.1016/j.jhydrol.2007.09.044.



- Overeem, A., A. Buishand, and I. Holleman (2009a), Extreme rainfall analysis and estimation of depth-duration-frequency curves using  
380 weather radar, *Water Resour. Res.*, 45, W10424, doi:10.1029/2009WR007869.
- Overeem, A., I. Holleman, and A. Buishand (2009b), Derivation of a 10 year radar-based climatology of rainfall, *J. Appl. Meteorol. Climatol.*,  
48, 1448–1463, doi:10.1175/2009JAMC1954.1.
- Overeem, A., T. A. Buishand, I. Holleman, and R. Uijlenhoet (2010), Extreme value modeling of areal rainfall from weather radar, *Water  
Resour. Res.*, 46, W09514, doi:10.1029/2009WR008517.
- 385 L. Panziera, M. Gabella, U. Germann and O. Martius, A 12-year radar-based climatology of daily and sub-daily extreme precipitation over  
the Swiss Alps, *International Journal of Climatology*, 38, 10, (3749-3769), (2018).
- Papalexiou, S.M. and Koutsoyiannis, D., 2013. Battle of extreme value distributions: A global survey on extreme daily rainfall. *Water  
Resources Research*, 49, 187–201. doi:10.1029/2012WR012557
- Paulitsch, H., Teschl, F., and Randeu, W. L.: Dual-polarization C-band weather radar algorithms for rain rate estimation and hydrometeor  
390 classification in an alpine region, *Adv. Geosci.*, 20, 3-8, <https://doi.org/10.5194/adgeo-20-3-2009>, 2009.
- Pavan, V., Antolini, G., Barbiero, R. et al. High resolution climate precipitation analysis for north-central Italy, 1961–2015. *Clim Dyn* 52,  
3435–3453 (2019) doi:10.1007/s00382-018-4337-6
- Peleg, Nadav and Marra, Francesco and Fatichi, Simone and Paschalis, Athanasios and Molnar, Peter and Burlando, Paolo. (2016). Spatial  
variability of extreme rainfall at radar subpixel scale. *Journal of Hydrology*. 10.1016/j.jhydrol.2016.05.033.
- 395 Ragulina, Galina and Reitan, Trond. (2017). Generalized extreme value shape parameter and its nature for extreme precipitation using long  
time series and the Bayesian approach. *Hydrological Sciences Journal*. 62. 1-17. 10.1080/02626667.2016.1260134.
- Reimel, K. J., and Kumjian, M., (2021). Evaluation of KDP Estimation Algorithm Performance in Rain Using a Known-Truth Framework,  
*Journal of Atmospheric and Oceanic Technology*, 38(3), 587-605. Retrieved Jun 15, 2021, from <https://journals.ametsoc.org/view/journals/atot/38/3/JTECH-D-20-0060.1.xml>
- 400 Ryzhkov, A.V., Schuur, T.J., Burgess, D.W., Heinselman, P.L., Giangrande, S.E. and Zrnich, D.S. (2005). The Joint Polarization Experiment:  
Polarimetric rainfall measurements and hydrometeor classification. *Bulletin of the American Meteorological Society*, 86(6), pp.809-824.
- Ryzhkov, A.V., Kumjian, M.R., Ganson, S.M. and Zhang, P. (2013). Polarimetric radar characteristics of melting hail. Part II: Practical  
implications. *Journal of Applied Meteorology and Climatology*, 52(12), pp.2871-2886.
- Schroeder, K., Kirchengast, G., and O, S. (2018). Strong dependence of extreme convective precipitation intensities on gauge network density.  
405 *Geophysical Research Letters*, 45, 8253– 8263. <https://doi.org/10.1029/2018GL077994>
- Tammets, T., and Jaagus, J. (2013). Climatology of precipitation extremes in Estonia using the method of moving precipitation totals.  
*Theoretical and Applied Climatology*, 111(3), 623-639.
- Voormansik, T., Cremonini, R., Post, P., and Moiseev, D.: Evaluation of the dual-polarization weather radar quantitative precipitation  
estimation using long-term datasets, *Hydrol. Earth Syst. Sci.*, 25, 1245–1258, <https://doi.org/10.5194/hess-25-1245-2021>, 2021a
- 410 Voormansik, T., Múirsepp, T., and Post, P.: Climatology of Convective Storms in Estonia from Radar Data and Severe Convective Environ-  
ments, *Remote Sens.*, 13(11), 2178, <https://doi.org/10.3390/rs13112178>, 2021b
- Vuerich, E., Monesi, C., Lanza, L., Stagi, L., Lanzinger, E.: WMO Field Intercomparison of Rainfall Intensity Gauges, Vigna di Valle, Italy,  
October 2007-April 2009, WMO/TD- No. 1504; IOM Report- No. 99, 2009.
- Gianfranco Vulpiani, Mario Montopoli, Luca Delli Passeri, Antonio G. Gioia, Pietro Giordano, and Frank S. Marzano, 2012: On the Use  
415 of Dual-Polarized C-Band Radar for Operational Rainfall Retrieval in Mountainous Areas. *J. Appl. Meteor. Climatol.*, 51, 405-425, doi:  
10.1175/JAMC-D-10-05024.1.



<https://doi.org/10.5194/amt-2022-220>  
Preprint. Discussion started: 5 August 2022  
© Author(s) 2022. CC BY 4.0 License.



Wang, Y. and V. Chandrasekar. (2009). Algorithm for Estimation of the Specific Differential Phase. *J. Atmos. Oceanic Technol.*, 26, 2565–2578, <https://doi.org/10.1175/2009JTECHA1358.1>

Wilks, Daniel S. *Statistical Methods in the Atmospheric Sciences*. 3rd ed. Oxford ; Waltham, MA: Academic Press, 2011.